



## A non-hydrostatic Rhea

R. A. Mackenzie,<sup>1,2</sup> L. Iess,<sup>3</sup> P. Tortora,<sup>4</sup> and N. J. Rappaport<sup>1</sup>

Received 5 December 2007; accepted 11 February 2008; published 14 March 2008.

[1] Radiometric data obtained during Cassini's close flyby of Rhea, on 26 November 2005, has been subject to several published analyses aiming to determine the satellite's mass and quadrupole gravity moments. Combining aspects of two of these analyses we present our best, unbiased estimates of the gravity field parameters and point out how the constraint of hydrostatic equilibrium adopted by previous analysts affects the results. We present solutions based on a broad range of geophysical assumptions, such as the presence of degree 3 and 4 gravity field constrained at different levels. The result is a balanced approach which describes our current knowledge of Rhea's gravity field. In the case of a gravity field limited to second degree harmonics the most reliable estimates are  $GM = 153.9398 \pm 0.0008 \text{ km}^3 \text{ s}^{-2}$ ,  $10^6 J_2 = 931.0 \pm 12.0$ ,  $10^6 C_{22} = 237.2 \pm 4.5$ , and  $10^6 S_{22} = 3.8 \pm 3.8$ . **Citation:** Mackenzie, R. A., L. Iess, P. Tortora, and N. J. Rappaport (2008), A non-hydrostatic Rhea, *Geophys. Res. Lett.*, 35, L05204, doi:10.1029/2007GL032898.

### 1. Introduction

[2] The determination of the gravity fields of the Saturnian satellites is one of the main scientific goals of the Cassini mission. On November 25, 2005, during an almost equatorial flyby with altitude 502 km, the Cassini spacecraft was tracked through its closest approach (C/A) with Rhea, allowing a determination of the gravity quadrupole field. The estimation was based on range and range-rate measurements obtained from a coherent radio link between the spacecraft and the antennas of the Deep Space Network (DSN). The data set was independently analyzed by Mackenzie *et al.* [2007] for the Cassini Navigation Team (NAV) and Iess *et al.* [2007] for the Cassini Radio Science Team (RS). Different solutions were derived as a result of distinct analysis approaches. However, these two results are here made compatible by merging the best aspects of each approach. A third set of values was also recently published by Anderson and Schubert [2007], based on a preliminary inter-office memorandum by R. A. Mackenzie *et al.* (Cassini Rhea-1 flyby—Results of Rhea gravity observation, Jet Propulsion Laboratory, 2006) issued by NAV just after the radiometric data acquisition, where many solution sensitivities were examined. By selecting one of the solutions presented in this memo, strongly constrained a priori to hydrostatic equilibrium, values for  $J_2$  and  $C_{22}$  were pub-

lished by Anderson and Schubert [2007]. Based on these values, an interior model for an undifferentiated Rhea, consisting of a homogeneous mix of rock and ice, was presented.

[3] With a single flyby, the determination of the gravity field is possible only if some geophysical assumptions are made. Anderson and Schubert [2007] assumed a hydrostatically constrained quadrupole field. Mackenzie *et al.* [2007] and Iess *et al.* [2007] estimated an unconstrained quadrupole field. Other possible approaches include allowing the presence of a significant higher degree field or the possibility of reorientation as a result of impacts. The assumptions adopted by Anderson and Schubert [2007] are by far the most stringent and severely limit any subsequent interpretation.

[4] The motivation for the present paper is a critical assessment of the present knowledge of Rhea's quadrupole coefficients, as these values represent crucial quantities for the determination of realistic interior models. This paper presents a re-analysis of Rhea's radiometric tracking data by NAV and RS to compute the best unbiased values of  $GM$ ,  $J_2$  and  $C_{22}$  and examines the solution sensitivities to a priori assumptions.

### 2. Summary of Previous Analyses

[5] The NAV approach published by Mackenzie *et al.* [2007] examines a number of solution sensitivities. These include the sensitivity to the data arc span, to the application of a priori hydrostatic constraints and to the Doppler data weighting scheme. The estimated parameters are the spacecraft state, the magnitude and direction of spacecraft thrusting events, the states and GMs of Saturn and all its main satellites, and the  $J_2$ ,  $C_{22}$  and  $S_{22}$  of Rhea. Optical navigation images of the satellites complement the radiometric X-band up, X-band down (X/X-band) range and Doppler, which are corrected with standard ionosphere and troposphere calibrations. Data weighting schemes account for expected low frequency plasma perturbations by either de-weighting the Doppler data or by applying a Doppler pre-whitening algorithm. In the case at hand, however, the use of a diagonal weighting matrix, whose elements are inversely proportional to the variance of the residuals, is equally acceptable, as the noise spectra are essentially white over the frequency band of interest. A priori covariance matrices for the spacecraft state and the states and GMs of the Saturnian system bodies are derived from previous orbit determination arc solutions, thereby providing information on the longer period dynamics. This approach provides a set of coefficients which are consistent with the best available orbit solution of Cassini relative to Rhea and Saturn. In the work of Mackenzie *et al.* [2007] it is recommended that the data arc should contain at least the tracking pass after Saturn pericenter, and the a priori hydrostatic constraint should not be applied since it degrades the Doppler fit at closest

<sup>1</sup>Jet Propulsion Laboratory, California Institute of Technology, Pasadena, California, USA.

<sup>2</sup>Now at European Space Operations Centre, Darmstadt, Germany.

<sup>3</sup>Dipartimento di Ingegneria Aerospaziale e Astronautica, Università di Roma "La Sapienza," Rome, Italy.

<sup>4</sup>DIEM, II Facoltà di Ingegneria, Università di Bologna, Forlì Italy.

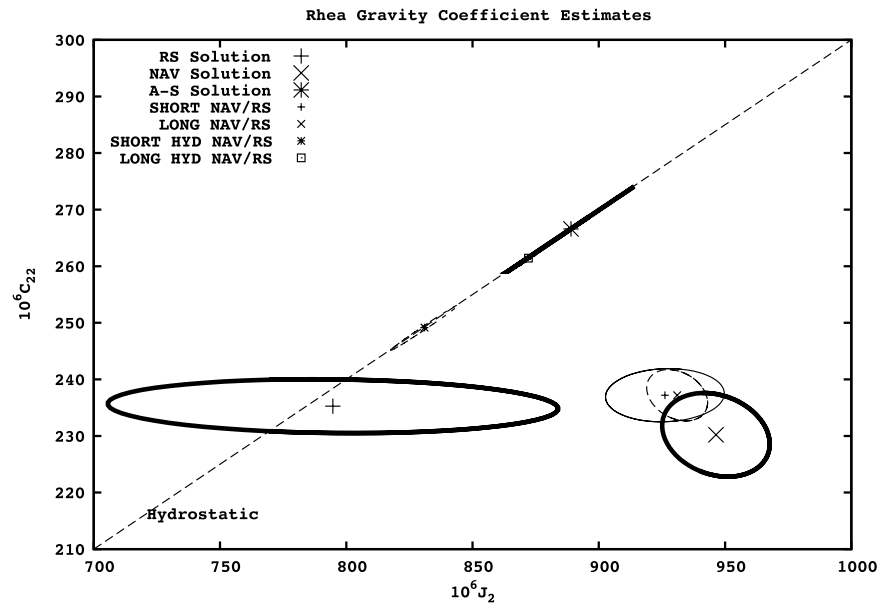


**Figure 1.** Estimated  $J_2$  versus  $C_{22}$  for Mackenzie *et al.* [2007], Jess *et al.* [2007], and Anderson and Schubert [2007] approaches. Also plotted is the combined NAV/RS solution with (LONG) and without (SHORT) the extra pass and with (HYD) and without the hydrostatic constraint applied a priori. The dotted line refers to the hydrostatic ratio  $J_2/C_{22} = 10/3$ .

approach. The preferred values and formal  $1\sigma$  uncertainties obtained are  $GM = 153.9403 \pm 0.0009 \text{ km}^3 \text{ s}^{-2}$ ,  $10^6 J_2 = 946.4 \pm 21.3$ ,  $10^6 C_{22} = 230.2 \pm 7.4$ , and  $10^6 S_{22} = 8.2 \pm 6.0$ . The dynamical model where Rhea's gravity field is limited to a degree 2 harmonics appears adequate, as the residuals have zero mean with a rms value fully compatible with the expected noise sources (mostly interplanetary plasma and wet troposphere). The formal uncertainties may be therefore assumed to be close to the true uncertainties. The main drawback of the analysis is that it does not use the less noisy X-band up, Ka-band down (X/Ka-band) Doppler data and the newer and more accurate advanced media calibration (AMC) troposphere data. The RS approach is intended as a refinement of the reconstructed orbit solution provided by the NAV team and involves analyzing a short data arc containing no maneuver. An arc of 24 hours is used, centered on the Rhea flyby and using only X/Ka Doppler data, corrected where possible with AMC data. The estimated parameters are the state of the spacecraft, the state and GM of Rhea and the gravity parameters of Rhea. The spacecraft and Rhea states are constrained without taking the orbit determination solution history into account and therefore a local fit to the Doppler data is obtained, largely unconstrained by the longer period dynamics. This approach has the advantage of using Doppler data which is less affected by solar plasma and ionospheric perturbations and uses superior tropospheric corrections, which is important since much of the Doppler data was obtained at low elevation angles. However, the AMC corrections were not available for the crucial closest approach data, forcing the use of the standard corrections for this pass. A disadvantage of this method is that it discards information about the Cassini and Rhea orbits by its choice of a priori constraints and it does not use the range data. Furthermore, the arc is rather short and may not contain sufficient change in geometry to allow a robust determination of the orbit

relative to Rhea. Despite the relative simplicity of the RS orbit determination the Rhea gravity parameters obtained by this study are in fairly good agreement with the NAV team values;  $GM = 153.9395 \pm 0.0018 \text{ km}^3 \text{ s}^{-2}$ ,  $10^6 J_2 = 794.7 \pm 89.2$ ,  $10^6 C_{22} = 235.3 \pm 4.8$ , and  $10^6 S_{22} = 3.07 \pm 4.39$ . The RS determined values of  $GM$  and  $C_{22}$  are consistent at the  $1\sigma$  level with the NAV team's results and at the  $2\sigma$  level for  $J_2$ .

[6] The third method was published by Anderson and Schubert [2007] and takes as a starting point a JPL inter-office memorandum prepared by Mackenzie *et al.* (2006). In this unpublished document, several solution sensitivities are studied, including an analysis aiming to check the consistency of the data with the a priori assumption of hydrostatic equilibrium. Solutions with and without a constraint forcing hydrostatic equilibrium are presented and a recommendation in favor of a solution using no a priori hydrostatic constraint is made. In the work of Anderson and Schubert [2007] a  $3 \times 3$  sub-matrix of the non-hydrostatic a posteriori covariance matrix, containing only the Rhea  $GM$ ,  $J_2$  and  $C_{22}$  terms, is constrained to hydrostatic equilibrium. The result is values of the quadrupole coefficients of  $GM = 153.9372 \pm 0.0013 \text{ km}^3 \text{ s}^{-2}$ ,  $10^6 J_2 = 889.0 \pm 25.0$ ,  $10^6 C_{22} = 266.6 \pm 7.5$ , values very close to those obtained by Mackenzie *et al.* (unpublished memorandum, 2006) for the application of the same constraint a priori. This approach is entirely based on theoretical predictions. Not surprisingly, the application of a hydrostatic constraint, analyzed by Mackenzie *et al.* [2007], leads to a significant degradation of the orbital fit around closest approach.

[7] The  $J_2$  and  $C_{22}$  values obtained in the three analyses are presented in Figure 1. The mean values are plotted on a  $J_2$ ,  $C_{22}$  plane with the  $1\sigma$  error ellipses, taking into account the a posteriori correlations. Also plotted is the hydrostatic equilibrium constraint  $3J_2 = 10C_{22}$ . Of the three, only the NAV solution shows significant departure from hydrostatic

equilibrium, although the RS study's determination of  $J_2$  is not sufficiently accurate to make a firm statement in that regard.

### 3. Convergence of Previous Analyses

[8] In order to understand the differences in their approaches and to present the best possible set of unbiased values the NAV and RS teams have compared their analyses in detail and combined their approaches to present an improved set of values. The X/Ka band Doppler data and AMC corrections are preferred to the X/X data and standard corrections and are used whenever available. The data weighting method of both teams is to use a pass by pass scheme. The NAV team approach of de-weighting the data relative to the rms is justified if the observed frequency spectrum of the Doppler data is dominated by the effects of solar plasma. This is judged not to be the case for the crucial closest approach pass, and it has been decided to weight by the rms of the pass. Starting from the RS solution, some features of the NAV solution were applied: range data are added and the spacecraft state parameters and the satellite parameters are constrained using the long term orbit determination solution history. Supplementing the fit with either of these additions results in a significant improvement in the estimation of  $J_2$ . The RS data arc is lengthened by one partial pass of range and X/X Doppler data after the Saturn pericenter, terminating just prior to an orbital maneuver. Adding the NAV solution features, the extra pass pre-fit residual mean is reduced from 0.25 to 0.01 Hz., a clear indication of an improved solution. Using the additional pass the solution becomes insensitive to the addition of the range data or the application of the NAV a priori constraints, and it is this robustness which gives confidence in our result. The final estimates are  $GM = 153.9398 \pm 0.0008 \text{ km}^3 \text{ s}^{-2}$ ,  $10^6 J_2 = 931.0 \pm 12.0$ ,  $10^6 C_{22} = 237.2 \pm 4.5$ , and  $10^6 S_{22} = 3.8 \pm 3.8$ . Figure 1 contains a summary of all solutions. The most accurate determination is obtained from the NAV/RS combined arc with the extra pass. The  $J_2$  value is changed by over  $1.5\sigma$  relative to the RS solution and towards the NAV solution. The value of  $C_{22}$  is closer to the RS solution but is changed by less than  $1\sigma$  relative to the NAV solution.

### 4. Applying a Hydrostatic Constraint

[9] When any additional constraint is applied to an orbit determination solution the residuals will necessarily be affected adversely. If the effect is significant, the constraint applied is not consistent with the data and/or the other assumptions made in the orbit determination. As part of the current analysis, we examine the effect on the data of applying an a priori hydrostatic constraint correlating the  $J_2$  and  $C_{22}$ , so that the relation  $3J_2 = 10C_{22}$  is assumed. In Figure 1, the hydrostatic solutions using the combined NAV/RS approach with and without the extra pass are plotted. In both solutions, the  $C_{22}$  estimate is moved significantly relative to the unconstrained solutions. The constrained solutions and their uncertainty ellipses lie along the hydrostatic line. For the shorter arc the  $C_{22}$  change is  $2\sigma$ , for the longer arc it is around  $4\sigma$ . The Doppler tracking residuals near C/A with and without the hydrostatic con-

straint are given in Figure 2. The hydrostatic solution results in a significant signature in the residuals around closest approach which is not present in the unconstrained solution. Quantitatively, the peak-to-peak variation of the frequency residuals from 23:45 to 23:55 UT increases from 17 mHz to 48 mHz when the hydrostatic constraint is applied, while the residuals outside this interval do not change appreciably. Such a large degradation of the fit near closest approach suggests a deviation from the hydrostatic  $J_2/C_{22}$  ratio.

### 5. Impact Basins and Higher Degree Field

[10] One mechanism which can produce a non-hydrostatic  $J_2/C_{22}$  is the formation of impact basins as a result of collisions occurring after the completion of the thermal evolution of the satellite, as described by *Nimmo and Matsuyama* [2007]. A large impact and the ensuing mass redistribution would change the orientation of the inertia ellipsoid, but after a suitable time internal dissipation will force a reorientation of the new principal axes toward the normal to the orbital plane and the empty focus of the orbit (almost coinciding with Saturn). This state corresponds to a minimum of the rotational energy. The tidal bulge is therefore no longer orientated toward Saturn. In the body fixed frame assumed in the orbit determination software, almost coinciding with the orbital frame, the values of  $J_2$  and  $C_{22}$  will be affected and the ratio  $J_2/C_{22}$  is no longer 10/3. *Nimmo and Matsuyama* [2007] have calculated the formation of the Tirawa basin on Rhea could have had this effect, resulting in a  $6.7^\circ$  reorientation of the satellite. In the pre-impact principal axes system the Tirawa basin, if uncompensated, would also produce a variation in  $J_2$  and  $C_{22}$  of 10–20%, besides generating a significant gravity anomaly. In this scenario the pre-impact values of  $J_2$  and  $C_{22}$  would have been different from the ones determined here, with important consequences for geophysical interpretation. Determination of the pre-impact quadrupole would require knowledge of Rhea's topography to account for the reorientation and the gravity anomaly produced by the basin.

[11] Also implicit in the approaches of both NAV and RS solutions is that the effect of higher degree and order coefficients on the flyby trajectory is negligible, even though a hydrostatic body's gravity field contains small degree four terms. To test the level at which this assumption affects the solution, we estimate a full non-hydrostatic  $4 \times 4$  gravity field. Such a field could be generated by internal convection or as a result of impact basins and craters. The  $1\sigma$  a priori uncertainties for the degree three and four normalized gravity coefficients are determined using Kaula's rule  $\bar{\sigma}_l = C \times 1.8 \times 10^{-3}/l^2$ . The value  $1.8 \times 10^{-3}$  is arbitrarily chosen so that  $\bar{\sigma}_2$  is equal to the normalized value of  $J_2$  when  $C = 1$ ,  $C$  being a scale factor controlling the permitted level of the higher degree field.

[12] Of course the value  $C = 1$  corresponds to a very large and unrealistic higher degree field, by comparison Kaula's rule for the moon [*Lemoine et al.*, 1997] is  $\bar{\sigma}_l = 1.5 \times 10^{-4}/l^2$ .

[13] Solutions are obtained using values of  $C$  ranging from very small to unity, ( $C = 0.001, 0.01, 0.05, 0.1, 0.5, 1$ ) and the results of the  $J_2$  and  $C_{22}$  estimation given in Figure 3. The combined NAV/RS solution is stable for  $C = 0.001$  and 0.01 but the solutions migrate in the  $J_2$ - $C_{22}$  plane from the

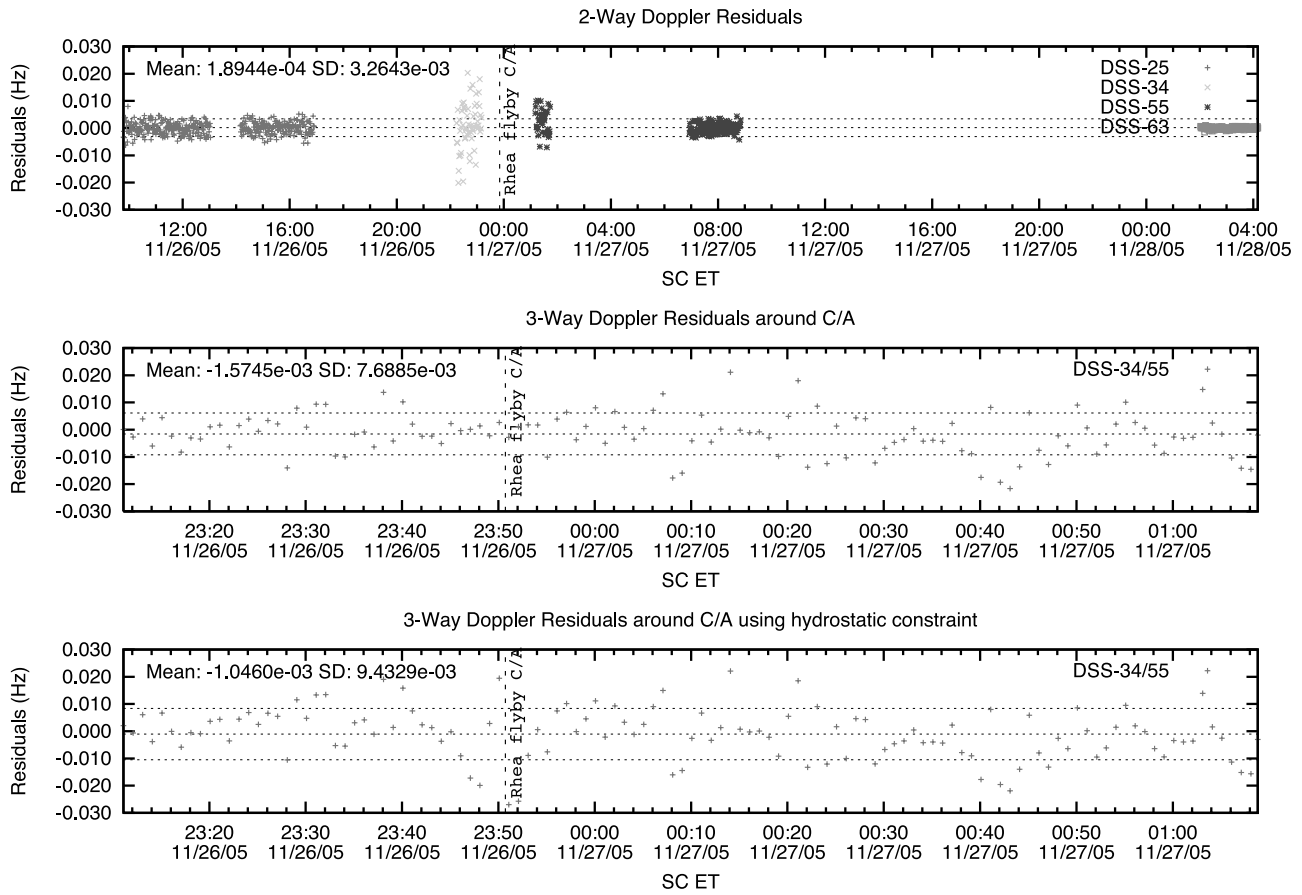


**Figure 2.** Tracking data residuals for the combined arc. Two- and three-way Doppler for the unconstrained arc and three-way Doppler for the hydrostatically constrained solution. The degradation of the residuals around closest approach for the hydrostatically constrained case is due to application of the hydrostatic constraint.

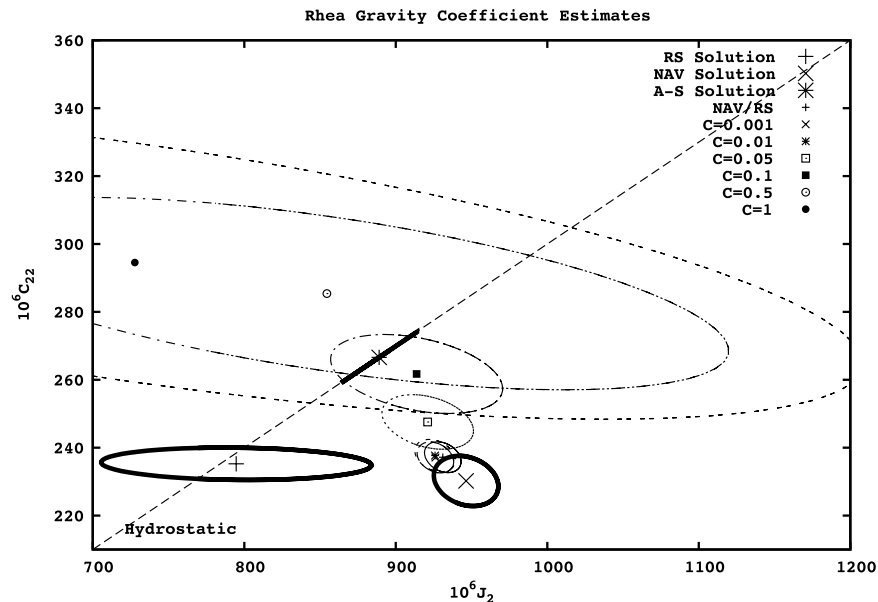


**Figure 3.** Estimated  $J_2$  versus  $C_{22}$  for cases estimating additional higher order gravity terms with varying a priori uncertainties for the degree three and four field. The dotted line refers to the hydrostatic ratio  $J_2/C_{22} = 10/3$ .

combined NAV/RS solution, generally towards and beyond the hydrostatically constrained solution but with increasing uncertainty ellipses. These uncertainties in the quadrupole moments reflect the increasing uncertainties in the higher degree terms. While the  $C = 0.1$ ,  $0.5$  and  $C = 1.0$  solutions are consistent with the hydrostatic solution the uncertainty ellipses are large, indicating that the quadrupole terms are not well determined. The estimates of the degree three and four terms are all around  $1\sigma$  or less, from their zero a priori. As expected, the Doppler residuals for all these cases show a better fit than the non-hydrostatic solution in Figure 2, and in particular no significant signature around closest approach.

[14] One may wonder which is the smallest  $l = 3$  field that would produce an appreciable degradation of the fit in a quadrupole only solution. Answering this question thoroughly would require extensive numerical simulations, a task beyond the scope of this paper. However an approximate upper limit to the higher degree field may be obtained by considering that in a solution limited to degree three harmonics, the smallest formal uncertainty associated to degree three (normalized) coefficients was found to be  $2.8 \times 10^{-5}$  ( $C_{33}$  and  $S_{33}$ ). Therefore one may argue that any unestimated coefficient larger than this formal uncertainty would affect the residuals at closest approach, therefore degrading the fit. Using this formal uncertainty as the largest allowed value of  $C_{33}$  and  $S_{33}$ , one derives an upper limit of 0.14 for the collocation parameter  $C$ .

## 6. Discussion

[15] The combined NAV/RS quadrupole only solution presented here is our best, unbiased estimate, assuming the higher degree field is negligible. This solution not only results in an excellent fit of the data, but, remarkably, is the one requiring the smallest set of parameters to produce such a fit. However, if Rhea has undergone any impact related reorientation these values must be interpreted with care since they include the direct effect of the impact basin and the fact that the tidal bulge is not orientated as predicted for an undisturbed body.

[16] There is a range of possible unbiased solutions for the quadrupole field which depend on how much uncertainty is placed a priori in the degree three and four terms of the Rhea gravity field. By varying the value of  $C$  one obtains a range of solutions for the quadrupole moments which has the NAV/RS solution at one end. By a suitable choice of  $C = 0.1$ , this unbiased approach can even produce a quadrupole field consistent with the hydrostatically constrained solution from Mackenzie et al. (unpublished memorandum, 2006).

[17] However, this assumes that a degree three field is present at a level consistent with a Kaula field  $\bar{\sigma}_l = 1.8 \times 10^{-4}/l^2$ , which may contradict the interpretation of homogeneity given by Anderson and Schubert [2007].

[18] Although the hydrostatic constraint biases the solution, therefore limiting its value, it is of some use from an analysis perspective. Applying the constraint reduces the

aliasing of any higher degree harmonics into the quadrupole field. However, the inability of the hydrostatic solution to fit the Doppler residuals around C/A is then evidence of the inadequacy of the gravity field model (see Figure 2). In addition, the uncertainties obtained in a purely hydrostatic solution do not take into account the presence of a higher degree field, and the strength of the constraint applied overwhelms any effect of the data, limiting the value of the method.

[19] Assuming that no impact related reorientation has occurred, we obtain a solution for the quadrupole moments  $GM = 153.9398 \pm 0.0008 \text{ km}^3 \text{ s}^{-2}$ ,  $10^6 J_2 = 931.0 \pm 12.0$ ,  $10^6 C_{22} = 237.2 \pm 4.5$ , and  $10^6 S_{22} = 3.8 \pm 3.8$ . Furthermore, we have evaluated the stability of the solution with respect to our a priori assumptions and have found that within a reasonable geophysical range of values, our solution is robust. Using a conservative upper bound of  $C < 0.05$  (corresponding to  $\bar{\sigma}_l < 9 \times 10^{-5}/l^2$ ) all solutions imply a non-hydrostatic quadrupole field with a ratio  $J_2/C_{22}$  between 3.7 and 3.9.

[20] Refinements of these values are possible if additional information is available. The figure and topography of Rhea would allow construction of an improved a priori gravity model and provide the orientation of the pre-impact ellipsoid. Impact basins and craters can be modeled as missing mass, whose value depends on an assumed correlation between gravity and topography. With additional flybys it may even be possible to determine a correlation factor which gives a consistent quadrupole field.

[21] **Acknowledgments.** The JPL part of this work was performed at the Jet Propulsion Laboratory, California Institute of Technology, under contract with NASA. The work of L. I. and P. T. was funded in part by the Italian Space Agency.

## References

- Anderson, J. D., and G. Schubert (2007), Saturn's satellite Rhea is a homogeneous mix of rock and ice, *Geophys. Res. Lett.*, *34*, L02202, doi:10.1029/2006GL028100.
- Iess, L., N. J. Rappaport, P. Tortora, J. Lunine, J. W. Armstrong, S. W. Asmar, L. Somenzi, and F. Zingoni (2007), Gravity field and interior of Rhea from Cassini data analysis, *Icarus*, *190*, 585–593.
- Lemoine, F. G. R., D. E. Smith, M. T. Zuber, G. A. Neumann, and D. D. Rolands (1997), A 70th degree lunar gravity model (GLGM-2) from Clementine and other tracking data, *J. Geophys. Res.*, *102*(E7), 16,339–16,359.
- Mackenzie, R. A. et al. (2007), A determination of Rhea's gravity field from Cassini navigation analysis, paper presented at 17th Space Flight Mechanics Meeting, Am. Astronaut. Soc., Sedona, Ariz..
- Nimmo, F., and I. Matsuyama (2007), Reorientation of icy satellites by impact basins, *Geophys. Res. Lett.*, *34*, L19203, doi:10.1029/2007GL030798.
- L. Iess, Dipartimento di Ingegneria Aerospaziale e Astronautica, Università di Roma "La Sapienza," via Eudossiana 18, I-00185 Rome, Italy.
- R. A. Mackenzie, European Space Operations Centre, Robert-Bosch Strasse 5, D-64293 Darmstadt, Germany. (ruaraidh.mackenzie@esa.int)
- N. J. Rappaport, Jet Propulsion Laboratory, California Institute of Technology, 4800 Oak Grove Drive, Pasadena, CA 91109, USA.
- P. Tortora, DIEM, II Facoltà di Ingegneria, Università di Bologna, via Fontanelle 40, Forlì, I-47100 Italy.